

Direct measurement of hot-spot temperature in flip-chip solder joints under current stressing using infrared microscopy

Hsiang-Yao Hsiao, S. W. Liang, Min-Feng Ku, Chih Chen, and Da-Jeng Yao

Citation: [Journal of Applied Physics](#) **104**, 033708 (2008); doi: 10.1063/1.2949279

View online: <http://dx.doi.org/10.1063/1.2949279>

View Table of Contents: <http://scitation.aip.org/content/aip/journal/jap/104/3?ver=pdfcov>

Published by the [AIP Publishing](#)

Articles you may be interested in

[Modeling of electromigration on void propagation at the interface between under bump metallization and intermetallic compound in flip-chip ball grid array solder joints](#)

J. Appl. Phys. **107**, 093526 (2010); 10.1063/1.3369442

[The time-dependent melting failure in flip chip lead-free solder interconnects under current stressing](#)

Appl. Phys. Lett. **93**, 041907 (2008); 10.1063/1.2963473

[Erratum: "Thermomigration in flip-chip SnPb solder joints under alternate current stressing" \[*Appl. Phys. Lett.*90, 152105 \(2007\)\]](#)

Appl. Phys. Lett. **90**, 249902 (2007); 10.1063/1.2748851

[Thermomigration in flip-chip SnPb solder joints under alternating current stressing](#)

Appl. Phys. Lett. **90**, 152105 (2007); 10.1063/1.2721136

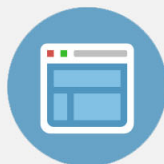
[Infrared microscopy of hot spots induced by Joule heating in flip-chip SnAg solder joints under accelerated electromigration](#)

Appl. Phys. Lett. **88**, 022110 (2006); 10.1063/1.2151255



Re-register for Table of Content Alerts

Create a profile.



Sign up today!



Direct measurement of hot-spot temperature in flip-chip solder joints under current stressing using infrared microscopy

Hsiang-Yao Hsiao,¹ S. W. Liang,¹ Min-Feng Ku,¹ Chih Chen,^{1,a)} and Da-Jeng Yao²

¹Department of Materials Science and Engineering, National Chiao Tung University, Hsin-chu 30010, Taiwan, Republic of China

²Institute of NanoEngineering and MicroSystem, National Tsing Hua University, Hsin-chu 300, Taiwan, Republic of China

(Received 10 February 2008; accepted 22 April 2008; published online 6 August 2008)

Several simulation studies reported that a hot spot exists in flip-chip solder bumps under accelerated electromigration. Yet, there are no experimental data to verify it. In this paper, the temperature distribution during electromigration in flip-chip SnAg3.5 solder bumps is directly inspected using infrared microscopy. Two clear hot spots are observed in the bump. One is located at the region with peak current density and the other one is at the bump edge under the current-feeding metallization on the chip side. Under a current stress of 1.06×10^4 A/cm², the temperature in the two hot spots are 161.7 and 167.8 °C, respectively, which surpass the average bump temperature of 150.5 °C. In addition, the effect of under-bump-metallization (UBM) thickness on the hot spots is also examined. It indicates that the hot-spot temperature in the solder bump increases for the solder joints with a thinner UBM. Electromigration test indicates that these hot spots have significant influence on the initial failure location. © 2008 American Institute of Physics. [DOI: 10.1063/1.2949279]

I. INTRODUCTION

Flip-chip technology has been adopted for high-density packaging due to its excellent electrical performance and better heat dissipation ability.¹ As the required performance in microelectronic devices becomes higher, the current that each bump needs to carry is 0.2 A, and it will increase to 0.4 A in the near future. Furthermore, to meet the miniaturization trend of portable devices, the dimensions of the solder bumps continue to shrink, causing the current density in each solder joint to increase abruptly. Therefore, electromigration in the solder bumps become an important issue.²

Several investigations on electromigration in flip-chip solder joints have been carried out.^{3–10} Current crowding effect occurs seriously near the entrance point of the Al trace into the solder joint, which is responsible for the failure in the chip/anode side of the solder joint.^{4,5} Furthermore, Joule heating effect also takes place during accelerated electromigration tests.^{6–10} During electromigration tests, the applied current may be as high as 2.2 A,³ which may cause serious Joule heating in the solder joints. The temperature increase due to current stressing may be over 30 °C when a 1.0 A current is applied to the solder bump.^{5–7} In addition, several simulation studies point out that there exists a hot spot in the solder bump near the entrance of the Al trace.^{7–9} On the other hand, Lai *et al.* showed that there is no such hot spot based on their simulation results.¹¹ The temperature may affect the mean time to failure (MTTF) significantly, as depicted by Black's equation:¹²

$$\text{MTTF} = A \frac{1}{j^n} \exp\left(\frac{Q}{kT}\right), \quad (1)$$

where A is a constant, j is the current density in A/cm², n is a model parameter for current density, Q is the activation energy, k is Boltzmann's constant, and T is the average bump temperature in kelvin. However, no experimental results have been reported to confirm the existence of the hot spot. This is because the solder joints are completely surrounded by a Si substrate, underfill, and a substrate. Thus it is difficult to investigate the hot-spot issue in solder joints.

To overcome this difficulty, the solder bump was polished first, and the temperature distribution inside the solder bump was measured by an infrared (IR) microscope at various stressing conditions. Hot spots were clearly observed at a high stressing current. Yet, there are no hot spots in the solder bump when the applied current density is lower than 3.5×10^3 A/cm². In addition, electromigration study was performed and the initial stage of failure was correlated with the hot spot.

II. EXPERIMENTAL

In order to investigate the hot-spot issue in flip-chip solder bumps, eutectic SnAg3.5 solder joints with typical dimensions were adopted. Figure 1 shows the cross-sectional scanning electron microscopy (SEM) image of the SnAg3.5 solder joint, which has a bump height of 70 μm and an under-bump-metallization (UBM) opening of 120 μm in diameter on the chip side. The UBM consists of 0.1 μm Ti/5.0 μm Cu/3.0 μm Ni. The intermetallic compound (IMC) of Ni₃Sn₄ is formed at the interfacial of the UBM and the solder. The joints were polished laterally to approximately their centers, and then the joints were examined by x-ray to measure the remaining conduction area on the UBM

^{a)}Author to whom correspondence should be addressed. Electronic mail: chih@mail.nctu.edu.tw.

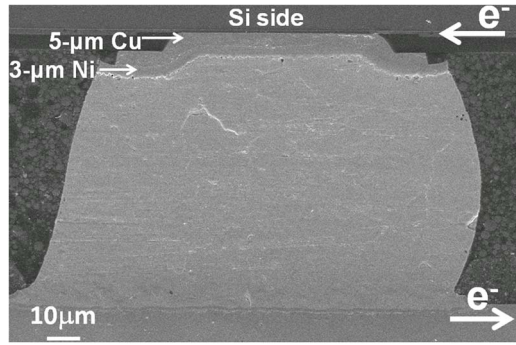


FIG. 1. (Color online) Cross-sectional SEM image for the SnAg solder bump before current stressing with a 5 μm Cu/3 μm Ni UBM. The electrons entered from the upper-right corner and left from the lower-right corner.

opening. The diameter of the solder joint is about 150 μm . The solder bumps were joined to an FR5 substrate. The original dimension of Al trace in the chip side was 100 μm wide and 1.5 μm thick, while the dimension of the Cu lines on the substrate was 25 μm thick and 100 μm wide. After polishing, the width of the Al trace and the Cu lines were also reduced to approximately 50% of their original values. The dimension of the Cu pad opening was 160 μm in diameter.

To observe the hot spot during current stressing, IR microscopy was employed. Prior to current stressing, the emissivity of the specimen was calibrated at 100 $^{\circ}\text{C}$. After calibration, the bumps were powered by a desired current. Then temperature measurement was performed to record the temperature distribution (map) at the steady state. The temperatures in the solder joints were mapped by a QFI thermal IR microscope, which has 0.1 $^{\circ}\text{C}$ temperature resolution and 2 μm spatial resolution. The surface microstructure changes were monitored with a SEM. Current stressing was carried out at a temperature of 100 $^{\circ}\text{C}$ on a hot plate. Current stress was applied to the bumps with the current density in the range of 1.77×10^3 – 1.06×10^4 A/cm² in the UBM opening.

III. SIMULATION

Three-dimensional finite element analysis (FEA) was performed to simulate the current-density distribution in the solder joint. The dimensions of the Al trace, pad opening, and Cu line were identical to those of the real flip-chip sample. The IMC formed between the UBM and the solder was also considered in the simulation models. The Ni layers on the chip and the substrate sides were assumed to consume 0.5 μm and form 1.0 μm of Ni₃Sn₄ IMC. Layered IMCs were used in this simulation for the Ni₃Sn₄ to avoid difficulty in meshization. In addition, eutectic SnAg solder was used in this model. The resistivity and thermal conductivity values of the materials used in the simulation are listed in Table I. The model used in this study was SOLID69 eight-node hexahedral coupled field element using ANSYS simulation software. The size of the element in the solder bump was 3.0 μm .

TABLE I. The properties of materials used in the simulation model.

| Materials | Resistivity at 20 $^{\circ}\text{C}$ |
|---------------------------------|--------------------------------------|
| Al trace | 3.2 |
| Electroless Ni | 70.0 |
| Cu | 1.7 |
| Electroplated Ni | 6.8 |
| SnAg solder | 12.3 |
| Ni ₃ Sn ₄ | 28.5 |

IV. RESULTS AND DISCUSSION

Hot spots start to emerge at a high density of approximately 3.5×10^3 A/cm². In this paper, we denote the existence of the hot spot when its temperature is 4.0 $^{\circ}\text{C}$ higher than the mean value in the solder bump, in which the mean temperature was obtained by averaging the values in a $50 \times 50 \mu\text{m}^2$ in the center of the bump. On the other hand, the hot-spot temperature was acquired by picking up the highest temperature in the region of interest. Figure 2(a) shows the

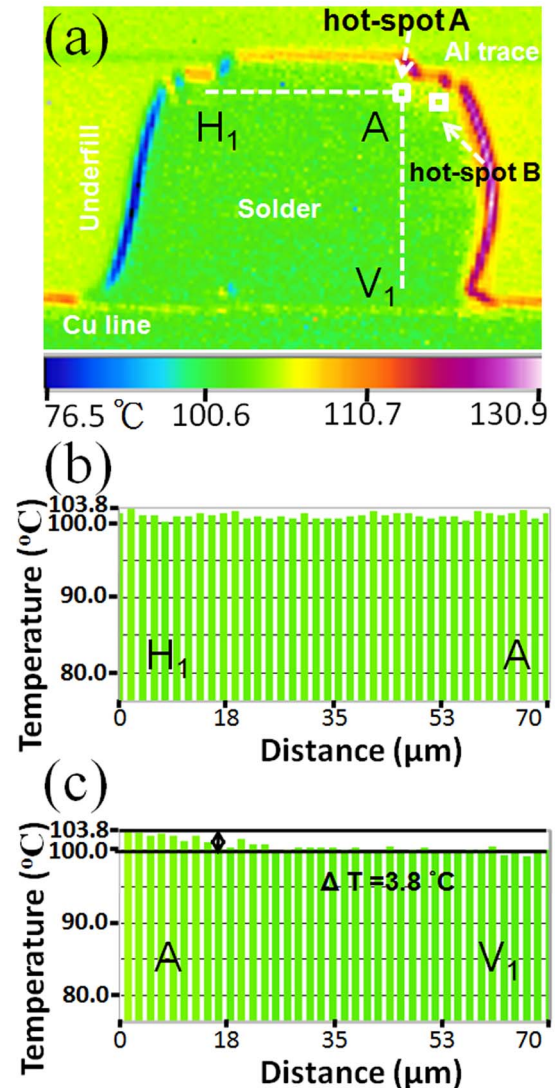


FIG. 2. (Color online) IR images showing the temperature distribution and the temperature profiles along the dashed lines in the SnAg bump with a 5 μm Cu/3 μm Ni UBM at 0.2 A.

temperature map distribution for the SnAg3.5 bump with a $5\ \mu\text{m}$ Cu/ $3\ \mu\text{m}$ Ni UBM during current stressing by $0.2\ \text{A}$. The temperature scale bar was shown in the x direction at the bottom of the figure. The current entered the solder bump through the Al trace on the chip end and it left the bump through the Cu line on the right-hand side of the substrate. The position of the Al trace is labeled in Fig. 2(a). The temperatures on the right and left edges of the bump may not be accurate since the image was taken at a prolonged exposure time of $15\ \text{s}$ and the sample may vibrate during the time span. The mean temperature in the bump was only $101.0\ ^\circ\text{C}$, which means that the average Joule heating was only $1.0\ ^\circ\text{C}$. However, there exists a hot spot in the solder bump. Figures 2(b) and 2(c) show the temperature profiles along the dashed horizontal AH_1 and vertical AV_1 lines in Fig. 2(a), respectively. The origin of Fig. 2(b) was set at point H_1 , whereas the origin of Fig. 2(c) was set at point A . The horizontal line is located in the solder right below the Ni_3Sn_4 layer. It shows that there is almost no temperature difference along the horizontal line, although there were small temperature fluctuations along the line. Since the temperature measurement by IR microscopy is very sensitive to surface roughness, the fluctuations may be due to surface roughness. However, there is about $3.8\ ^\circ\text{C}$ difference in temperature along the vertical line. The hot-spot temperature was $105.6\ ^\circ\text{C}$, which is located near the current entrance in the chip side into the bump. In this paper, this hot spot denote this location as hot spot A.

As the applied current is increased, the hot spot became more pronounced. Figure 3(a) illustrates the thermographs when the bump was subjected to a $0.4\ \text{A}$ current. A clear hot spot exists near the entrance of the current at the chip side. Figures 3(b) and 3(c) show the temperature profiles along the dashed horizontal AH_2 and vertical AV_2 lines in Fig. 3(a), respectively. The origin of Fig. 3(b) was set at point H_2 , whereas the origin of Fig. 3(c) was set at point A . The temperature difference increases to 4.6 and $9.0\ ^\circ\text{C}$ along the horizontal and vertical lines, respectively. When the stressing current is increased to $0.6\ \text{A}$, the hot spot became more significant, as depicted in Fig. 4(a). The horizontal temperature difference remains almost the same, whereas the vertical temperature difference continues to increase up to $16.7\ ^\circ\text{C}$, as illustrated in Figs. 4(b) and 4(c). The origin of Fig. 4(b) was set at point H_3 , whereas the origin of Fig. 4(c) was set at point A . A huge thermal gradient of $2392\ ^\circ\text{C}/\text{cm}$ is developed across the solder bump. The thermal gradient is defined here as the temperature difference between the two ends of the dashed line divided by the length of the line, which was $70\ \mu\text{m}$ for both the horizontal and vertical lines. The Joule heating effect also established a horizontal thermal gradient of $786\ ^\circ\text{C}/\text{cm}$.

Figure 5(a) shows the plot of average and hot-spot temperatures as a function of applied current densities/current with $5\ \mu\text{m}$ Cu/ $3\ \mu\text{m}$ Ni UBM. The applied current ranges from 0.1 to $0.6\ \text{A}$. With a higher current over $0.6\ \text{A}$, the solder bump may melt. The curve shows a parabolic behavior, which follows the Joule heating relationship:

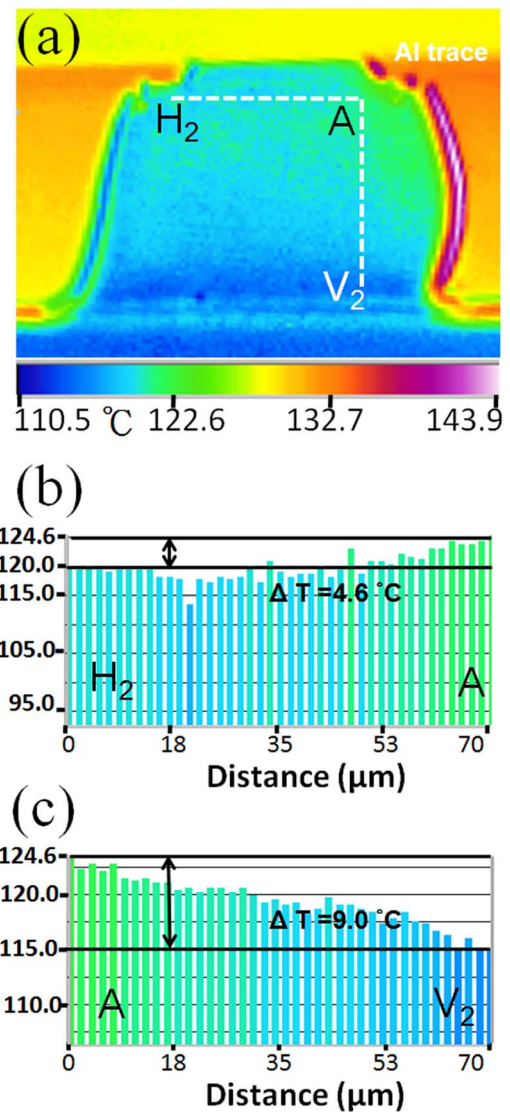


FIG. 3. (Color online) IR images showing the temperature distribution and the temperature profiles along the dashed lines in the SnAg bump with a $5\ \mu\text{m}$ Cu/ $3\ \mu\text{m}$ Ni UBM at $0.4\ \text{A}$.

$$P = I^2 R = J^2 \rho v, \quad (2)$$

where P is the heating power, I is the applied current, R is the resistance of the stressing circuit, j is the local current density, ρ is the resistivity, and v is the volume. In addition, the temperature difference between the average and hot-spot values becomes higher at a higher stressing current, which may be attributed to serious local Joule heating at the hot spot.

Three-dimensional FEA was carried out to correlate the local current density and the measured temperature and the simulation results are shown in Fig. 6. The electron flow entered the joint from the right-upper Al trace and left from the right-lower Cu line. The average current density is $1.10 \times 10^4\ \text{A}/\text{cm}^2$ when the joint was applied by $0.6\ \text{A}$. Yet, the local current density was about $2.46 \times 10^4\ \text{A}/\text{cm}^2$ inside the square near the entrance point of the Al trace, as labeled in the figure. This location matches hot spot A in the experimental results. At lower applied currents, the Al trace plays a key role on the Joule heating of the solder bump since it

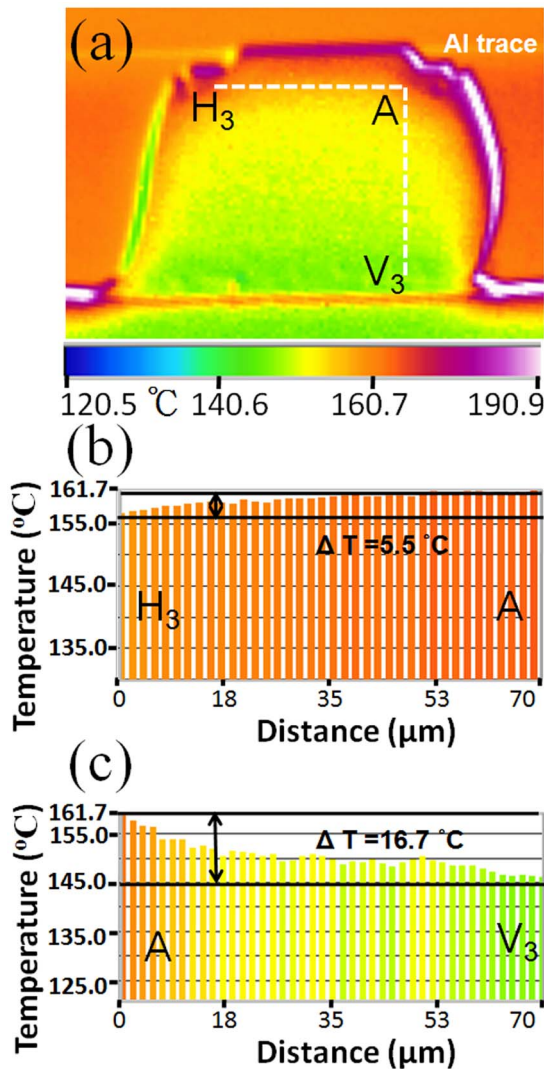


FIG. 4. (Color online) IR images showing the temperature distribution and the temperature profiles along the dashed lines in the SnAg bump with a 5 μm Cu/3 μm Ni UBM at 0.6 A.

connects the solder bumps and the current density in it reached $1.3 \times 10^5 \text{ A/cm}^2$ at 0.1 A. The resistance of the Al trace was measured to be 633 m Ω using four-point probes, whereas the resistance of each bump is only about 7 m Ω . The local current density was only $4.2 \times 10^3 \text{ A/cm}^2$ at 0.1 A in a $9 \mu\text{m}^3$ solder volume near the current entrance in the chip side. As the applied current increases, the local current density may start to contribute to Joule heating, and thus the hot spots emerge when the applied current is higher than 0.2 A.

It is interesting that as the applied current increases, the vertical thermal gradient increases faster than that of the horizontal thermal gradient, as depicted in Fig. 5(b). As shown in Figs. 2–4, the horizontal temperature differences are 4.5 and 5.5 $^\circ\text{C}$ for the 0.4 to 0.6 A, respectively, whereas the vertical temperature differences increase from 9.0 to 16.7 $^\circ\text{C}$ as the applied current increases from 0.4 to 0.6 A. It appears that the horizontal thermal gradient did not increase much after 0.3 A. This may be attributed to the fact that the lateral heat conduction is better than that of the vertical direction since Si has good heat dissipation abil-

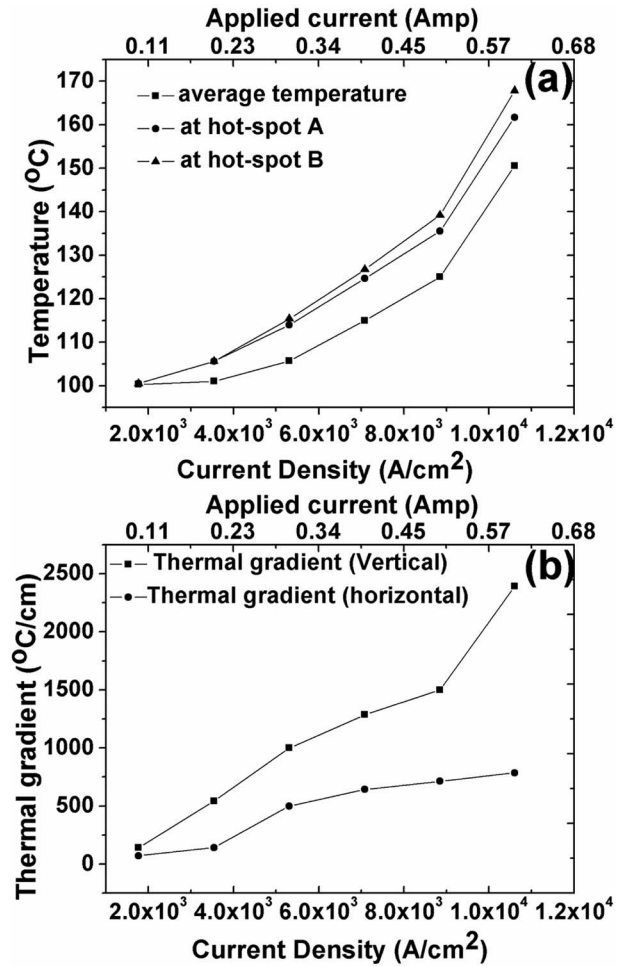


FIG. 5. (a) Temperature increases in the hot-spot region and in the bump as a function of applied current with a 5 μm Cu/3 μm Ni UBM. (b) Horizontal and vertical thermal gradients as a function of applied current with a 5 μm Cu/3 μm Ni UBM.

ity. From the analysis by a one-dimensional lumped model shown in Fig. 7, the vertical thermal resistance is 142.0 $^\circ\text{C/W}$, whereas the lateral thermal resistance is only 23.5 $^\circ\text{C/W}$. Therefore, the vertical thermal gradient appears to be much higher than that of the horizontal value. Accord-

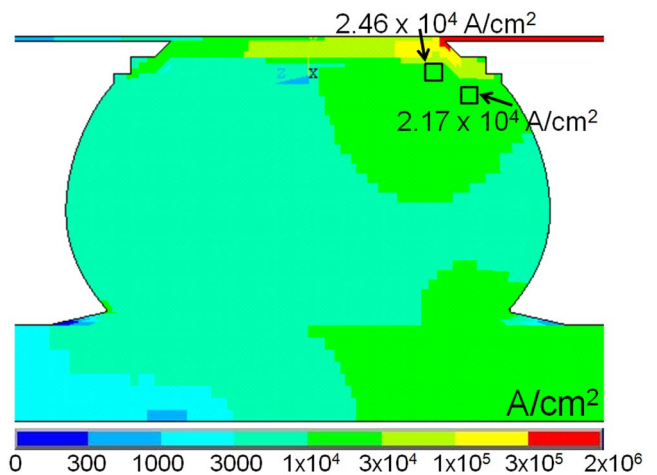


FIG. 6. (Color online) Simulated current-density distribution in the solder joint when powered by 0.6 A.

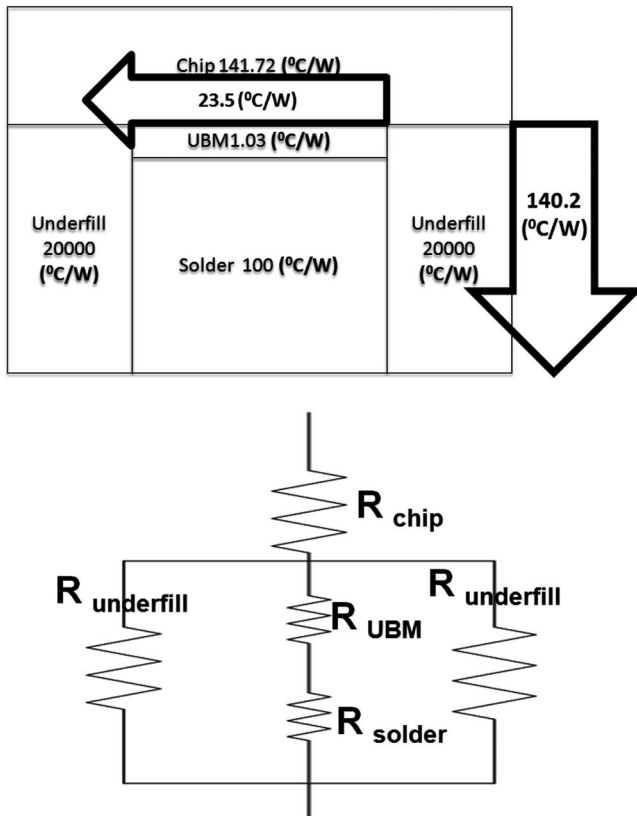


FIG. 7. One-dimensional lumped resistance model showing that the lateral thermal resistance is smaller than the vertical one.

ing to the analysis by Huang *et al.*,¹³ a thermal gradient larger than $1000\text{ }^{\circ}\text{C}/\text{cm}$ is needed in order to observe thermomigration during electromigration. As shown in Fig. 5(b), the horizontal gradient is always below this value. Thus, no lateral thermomigration has been reported up to date. Yet, the vertical gradient may reach this critical value at a higher applied current, resulting in a vertical thermomigration behavior.^{7,10,13}

Furthermore, it is surprising that there is another region with a lower local current density but possessed a temperature higher than the hot-spot value described above. The region is located in the right-hand side of the hot spot and close to the underfill, as marked by one of the white squares in Fig. 2(a). This region is denoted as hot spot B in this paper. The three-dimensional electrical simulation in Fig. 6 shows that the local current density is $2.17 \times 10^4\text{ A}/\text{cm}^2$, which is slightly lower than the value of $2.46 \times 10^4\text{ A}/\text{cm}^2$ in the region with peak current density. However, the average temperature there was as high as $167.8\text{ }^{\circ}\text{C}$, which is slightly higher than that at the hot spot with the maximum current density. The origin of this second hot spot may be attributed to two reasons: This region locates close to the Al trace, which serves as the major heating source in the joints. Secondly, it is adjacent to the underfill, which has a much higher temperature than the solder bump, since the heat dissipation ability is the worst among the materials in the joints. The average temperature for the underfill close to the Al trace was as high as $179.2\text{ }^{\circ}\text{C}$. Hence, the solder adjacent to the underfill may possess a higher temperature, although it has lower local Joule heating.

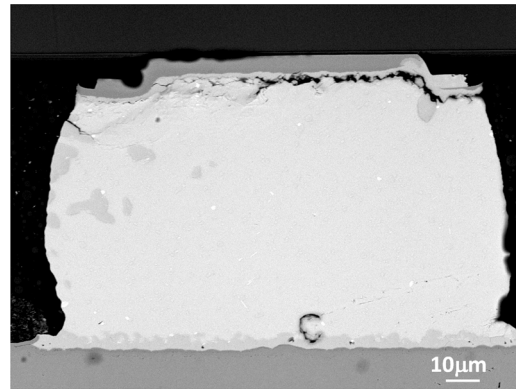


FIG. 8. (Color online) Cross-sectional backscattered SEM image showing the failure site for the solder joints stressed by 0.9 A at $150\text{ }^{\circ}\text{C}$ for 162 h .

In addition to current crowding effect, these hot spots may play a key role in the initial failure of solder bump during electromigration. Figure 8 shows the initial electromigration failure when another set of complete solder joints was stressed by 0.9 A at $150\text{ }^{\circ}\text{C}$ for 162 h . Under this stressing condition, the consumption of UBM appears to be the failure mechanism. The Ni UBM reacts with the solder to form Ni_3Sn_4 IMC. When Ni UBM is consumed, the solder would react with Cu UBM rapidly, leading to void formation in the passivation opening. Although the local current density at hot spot A is higher than that at hot spot B, it is often observed that the initial failure site also occurs at hot-spot B. The diffusion near the hot spot regions is faster and the dissolution rate of Ni and Cu UBMs is higher. As shown in Fig. 8, the Ni and Cu layers were consumed completely and formed Cu–Ni–Sn IMCs near the two hot spots. Therefore, hot spot B also plays a critical role on the initial electromigration failure for flip-chip solder joints.

V. CONCLUSION

In summary, two distinguished hot spots were observed in the bump when the applied current density is higher than $3.5 \times 10^3\text{ A}/\text{cm}^2$ for the solder joints used in this study. Two significant hot spots have been found: one at the region with peak current density and the other one at the bump edge under the current-feeding metallization on the chip side. It is surprising that the latter has an even higher temperature than the former. In addition, this hot spot B has significant influence on the initial failure site of electromigration. The dissolution rate of Cu/Ni UBM is faster near hot spot B; thus the joint starts to fail there.

ACKNOWLEDGMENT

The authors would like to thank the National Science Council of the Republic of China for financial support through Grant No. 95-2221-E-009-088MY3.

¹K. N. Tu, *J. Appl. Phys.* **94**, 5451 (2003).

²International Technology Roadmap for Semiconductors, Semiconductor Industry Association, San Jose, CA, 2003.

³C. Y. Liu, C. Chen, C. N. Liao, and K. N. Tu, *Appl. Phys. Lett.* **75**, 58 (1999).

⁴E. C. C. Yeh, W. J. Choi, and K. N. Tu, *Appl. Phys. Lett.* **80**, 4 (2002).

⁵T. L. Shao, Y. H. Chen, S. H. Chiu, and C. Chen, *J. Appl. Phys.* **96**, 4518

(2004).

⁶W. J. Choi, E. C. C. Yeh, and K. N. Tu, *J. Appl. Phys.* **94**, 5665 (2003).

⁷H. Ye, C. Basaran, and D. Hopkins, *Appl. Phys. Lett.* **82**, 7 (2003).

⁸S. H. Chiu, T. L. Shao, and C. Chen, *Appl. Phys. Lett.* **88**, 022110 (2006).

⁹S. W. Liang, Y. W. Chang, and C. Chen, *Appl. Phys. Lett.* **88**, 172108 (2006).

¹⁰H. Y. Hsiao and C. Chen, *Appl. Phys. Lett.* **90**, 152105 (2007).

¹¹Y.-S. Lai, K. M. Chen, C. L. Kao, C. W. Lee, and Y. T. Chiu, *Microelectron. Reliab.* **47**, 1273 (2007).

¹²J. R. Black, *IEEE Trans. Electron Devices* **16**, 338 (1969).

¹³A. T. Huang, A. M. Gusak, and K. N. Tu, *Appl. Phys. Lett.* **88**, 141911 (2006).